

## Freezing Behavior of a Water Droplet on a Rough Hydrophobic Surface Coated with a Short-chained Fluoroalkylsilane

Tsutomu Furuta,<sup>1,2</sup> Munetoshi Sakai,<sup>2</sup> Toshihiro Isobe,<sup>1</sup> and Akira Nakajima<sup>\*1,2</sup>

<sup>1</sup>Department of Metallurgy and Ceramics Science, Graduate School of Science and Engineering, Tokyo Institute of Technology, 2-12-1 O-okayama, Meguro-ku, Tokyo 152-8552

<sup>2</sup>Kanagawa Academy of Science and Technology,

308 East, Kanagawa Science Park, 3-2-1 Sakado, Takatsu-ku, Kawasaki, Kanagawa 213-0012

(Received July 14, 2010; CL-100630; E-mail: anakajim@ceram.titech.ac.jp)

A highly hydrophobic surface with nanoscale roughness was prepared by coating with a short-chained fluoroalkylsilane. The freezing behavior of a water droplet on the surface was then investigated. Freezing initiated in the vicinity of the three-phase contact line, producing a sharpened onion-like top on the droplet. The result of the freezing ratio at each time and the volume ratio at each height demonstrates the possibility that freezing advanced linearly in a vertical direction.

Highly hydrophobic surfaces are well known to be obtainable through a combination of methods to roughen the surface and lower the surface energy. The superior water-shedding property of highly hydrophobic surfaces is attributed to the presence of air at the solid–liquid interface because of the surface roughness.<sup>1</sup> The mechanism for this phenomenon is commonly called Cassie's mode.<sup>2</sup> When the rough surfaces are prepared from inorganic materials, surface treatment to lower the surface energy using organic compounds such as fluoroalkylsilane is usually necessary.

In a previous report, we described processing of a transparent coating with nanoscale roughness using boehmite and a sublimation agent.<sup>3</sup> Various highly hydrophobic surfaces are obtainable by coating with fluoroalkylsilane. Very recently, it was revealed that the stability of hydrophobicity on a fluoroalkylsilane surface at low temperature depends on the length of the fluorocarbon moiety in the top coating. When a short-chained fluoroalkylsilane such as FAS-3 ( $\text{CF}_3(\text{CH}_2)_2\text{Si}(\text{OCH}_3)_3$ ) is used, the wetting mode transition from Cassie's mode to Wenzel's mode,<sup>4</sup> which is water penetration into the rough surface structure, increases much greater with decreasing surface temperature than when a long-chained fluoroalkylsilane such as FAS-17 ( $\text{CF}_3(\text{CF}_2)_7(\text{CH}_2)_2\text{Si}(\text{OCH}_3)_3$ ) is used.<sup>5</sup>

On the other hand, various studies have been performed to elucidate the freezing of a water droplet on hydrophobic surfaces from the viewpoint of application to antifreezing coatings. The effect of the interaction between fluorine atoms in fluorocarbon and water molecules<sup>6,7</sup> and the effect of heat-transfer inhibition by air at the solid–liquid interface<sup>8</sup> have been investigated. However, reports of studies using direct observation and analysis of droplet-shape changes during freezing are limited. For this study, we investigated the freezing behavior of water droplets on highly hydrophobic surfaces with nanoscale roughness.

A commercial boehmite powder (AlOOH, 50 mg, DISPAL 18N4; Contec Co., Ltd., Hamburg, Germany) and reagent-grade acetylacetonate (AACA, 0.915 g,  $\text{Al}(\text{C}_5\text{H}_7\text{O}_2)_3$ , Tokyo Kasei Kogyo Co., Ltd., Tokyo, Japan) were mixed with ethanol (25 g).

The suspension was sonicated for 40 min. The suspension was coated onto a Si(100) wafer (cut to  $50 \times 50$  mm; Aki Corp., Miyagi, Japan) by spin coating at 1000 rpm for 10 s. The coated wafer was dried at room temperature for a few minutes. The wafer was then heated on a hot plate at 460 °C for 20 s. These coating and heating procedures were repeated five times to produce a surface with nanoscale roughness.

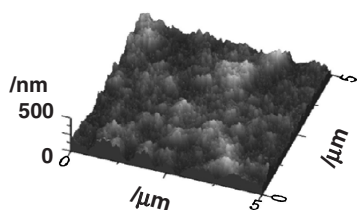
The coated plates were cleaned using vacuum ultraviolet light irradiation (VUV, 172 nm wavelength, UER-20; Ushio Inc., Tokyo, Japan) for 15 min in air at room temperature. These pre-cleaned plates were coated with fluoroalkylsilanes using chemical vapor deposition by heating together with  $0.02 \text{ cm}^3$  of either trifluoropropyltrimethoxysilane (FAS-3, KBM-7103; Shin-Etsu Chemical Co., Ltd., Tokyo, Japan) or 1H,1H,2H,2H-perfluorodecyltrimethoxysilane (FAS-17, TSL8233; GE Toshiba Silicones, Tokyo, Japan) in a Petri dish at 150 °C for 60 min (FAS-17) or 100 °C for 90 min (FAS-3) under flowing  $\text{N}_2$ . Then, before drying, the sample surfaces were rinsed using acetone, toluene, and distilled water.

Surface roughness ( $R_a$ ) was evaluated in a  $5 \times 5 \mu\text{m}$  area using an atomic force microscope (AFM, JSPM-4200; JEOL, Tokyo, Japan) with a Si cantilever (NSC36-c;  $\mu$ -masch, Narva Mtn., Estonia). Surface roughness ( $R_a$ ) and the roughness factor ( $r$ , the ratio of the actual area of a rough surface to the geometrically projected area) were obtained using surface analysis software (WinSPM Data Processing 2.15; JEOL, Tokyo, Japan) of the AFM. The static contact angle of 3- $\mu\text{L}$  water droplets was measured at five points using a contact angle meter (Dropmaster 500; Kyowa Interface Science Co., Ltd., Saitama, Japan) with the sessile drop method.

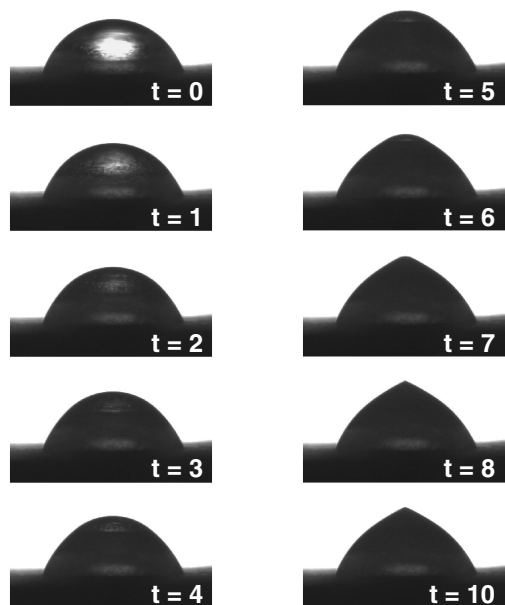
For the observation of the freezing behavior of water droplets, a Peltier cooling system (10021; Japan High Tech Co., Ltd., Fukuoka, Japan) was attached to the sample stage on the contact angle meter described above. The sample surface temperature was set to  $-12.0$  °C, and a 3.0  $\mu\text{L}$  distilled-water droplet ( $22.5$  °C) was placed on the sample surface. The shape change of the droplet was observed every 1.0 s. Atmospheric conditions for these measurements were  $22.5$  °C and 30% relative humidity.

Figure 1 portrays an AFM image of the prepared hydrophobic surface coated with FAS-3. Surface roughness ( $R_a$ ) and the roughness factor ( $r$ ) values of this sample were, respectively, 48 nm and 1.41. The static contact angle was  $146^\circ$  (average)  $\pm 2^\circ$  (standard deviation). The static contact angle of FAS-17-coated sample was  $160^\circ \pm 2^\circ$  (an AFM image of this sample is presented in Supporting Information<sup>9</sup>).

When the temperature on the FAS-17-coated surface was  $-12.0$  °C and a water droplet was placed on the sample surface,



**Figure 1.** AFM micrographs of the hydrophobic surface coated with FAS-3.



**Figure 2.** Freezing behavior of water droplet on the FAS-3-coated surface. The surface temperature was  $-12\text{ }^{\circ}\text{C}$ .

the droplet was not frozen; the contact angle was decreased slightly by dew condensation. On the other hand, for the FAS-3-coated surface, the droplet was frozen as soon as it was placed on the surface. The shape at the top of the droplet was sharpened like an onion upon the completion of freezing (Figure 2). For the FAS-3-coated surface, the wetting mode transition and resultant decrease of the amount of air phase at the solid–liquid interface were more remarkable than the FAS-17-coated surface with decreasing temperature.<sup>5</sup> It is deduced then that differences of heat transfer by the air phase<sup>8</sup> and the number of heterogeneous nucleation sites (solid–liquid interface) engenders the freezing behavior difference between these two silanes. Additionally, as pointed out by Suzuki et al.,<sup>7</sup> the difference of the interaction between fluorine atoms in the fluorocarbon moiety and water molecules might also affect the overall result. However, it has been difficult to evaluate the contributions from these effects independently to date. This point shall be addressed in future studies.

Figure 3 portrays the shape change of water droplet in during freezing on the FAS-3-coated surface. The  $x$  axis shows the elapsed time from the moment when the droplet was placed on the surface. The left axis shows the length of the contact radius ( $\Delta$ ) and the height ( $\square$ ) of the droplet; the right axis shows the droplet volume ( $\bullet$ ). The volume change of the droplet during

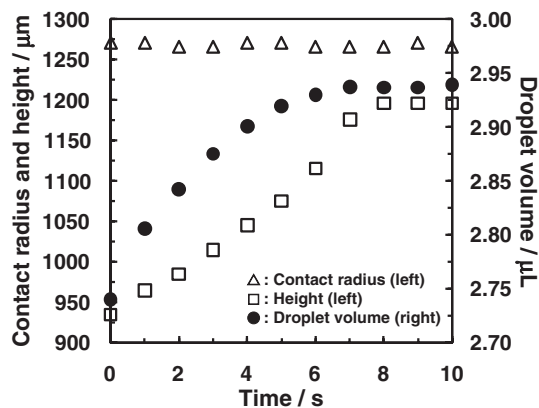


**Figure 3.** Time dependence of the shape change of water droplet in the freezing process at  $-12\text{ }^{\circ}\text{C}$  on the FAS-3-coated surface: contact radius ( $\Delta$ , left axis), droplet height ( $\square$ , left axis), and droplet volume ( $\bullet$ , right axis).

freezing was evaluated from the observed images at each time. First, outline extraction was performed from the binary image of the droplet using the image analysis system (DIP-Macro; Ditect Co., Ltd., Tokyo, Japan, the image of outline extraction is presented in Supporting Information<sup>9</sup>). The droplet volume was calculated from obtained coordinate data by rotational integration toward the  $y$  axis using sectional measurement. The circular shape of the droplet before and after freezing from the top-view was confirmed through direct observation. From Figure 3, the droplet height and volume increased concomitantly with the advance of freezing; however, the contact radius was almost constant. The freezing of the droplet was completed in around 8 s. From the volume change, the droplet density at the completion of the freezing ( $t = 8$  s) became about 0.93 times that of the initial droplet density ( $t = 0$  s). The theoretical value calculated from the density of liquid  $\text{H}_2\text{O}$  at  $22.5\text{ }^{\circ}\text{C}$  ( $0.998\text{ g cm}^{-3}$ ) and that of solid  $\text{H}_2\text{O}$  at  $0\text{ }^{\circ}\text{C}$  ( $0.917\text{ g cm}^{-3}$ ) was presumed as about 0.92. The theoretical value was almost identical to the experimental value. Consequently, results suggest that the droplet mass change was negligible during freezing.

When the droplet volumes of water (liquid  $\text{H}_2\text{O}$ ) and ice (solid  $\text{H}_2\text{O}$ ) are described as  $V_W$  ( $t = 0$  s) and  $V_I$  ( $t = 8$  s) respectively, the entire droplet volume at a certain time ( $V_t$ ) is obtainable using the freezing ratio ( $f, \leq 1$ ):

$$V_t = f \cdot V_I + (1 - f) \cdot V_W \quad (1)$$

Reforming eq 1, it is feasible to estimate the freezing ratio as follows.

$$f = \frac{V_t - V_W}{V_I - V_W} \quad (2)$$

Moreover, we calculated the integrated volume from solid–liquid interface to a certain height from the droplet shape at the completion of the freezing ( $t = 8$  s). The volume ratio at each height was obtained using the value of the integrated volume/ $V_I$  ( $t = 8$  s). The details of this calculation are presented in Supporting Information.<sup>9</sup>

Figure 4 portrays the obtained volume ratio at each height and the freezing ratio calculated from using eq 1 at each time on

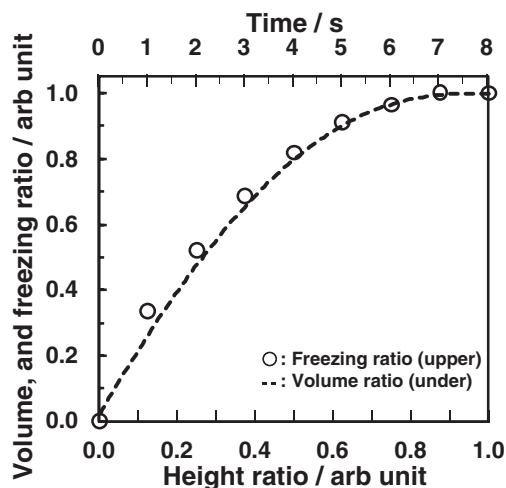


**Figure 4.** Volume ratio at each height (—, under  $x$  axis) and the freezing ratio at each time (○, upper  $x$  axis) in the freezing process at  $-12\text{ }^{\circ}\text{C}$  on the FAS-3-coated surface.

the FAS-3-coated surface. The  $y$  axis shows the volume ratio (—, dotted line) and the freezing ratio (○) of the droplet, the under  $x$  axis shows that the height ratio (the top of the droplet is 1.0; the bottom is 0.0), and the upper  $x$  axis shows the elapsed time. This shows that the freezing ratio at each time nearly corresponded to the volume ratio at each height suggesting that the freezing initiates from the solid–liquid interface and advanced to the droplet side in series. Moreover, it is conceivable that freezing of the droplet was advanced in the vertical direction almost linearly because the trends against elapsed time and height ratio corresponded.

As can be seen in Figures 3 and 4, it was rationalized that the freezing advanced from the solid–liquid interface to the top of the droplet with a constant contact radius value. Moreover, observation of the shape before and after freezing (Figure 5a) revealed that the shape of the droplet changed symmetrically during freezing. The contact radius of the droplet should increase if the freezing initiates concentrically from a central position of the solid–liquid interface. Alternatively, if the freezing starts from a dissymmetric position in the solid–liquid interface, then the shape of the droplet would not maintain symmetry because of anisotropic volume expansion. These arguments suggest that freezing initiates from the three-phase contact line (solid–liquid–vapor interface) and that the volume expansion advanced to the top of the droplet by fixing the three-phase contact line (Figure 5b). Suzuki et al. observed a droplet freezing on a smooth silane coating directly and reported that the freezing occurred from the three-phase contact line.<sup>7</sup> Our experimental results correspond to their observation.

In this study, a highly hydrophobic surface with nanoscale roughness was prepared by coating it with a short-chained fluoroalkylsilane, FAS-3. The freezing behavior of a water droplet on this surface was then investigated. When the surface

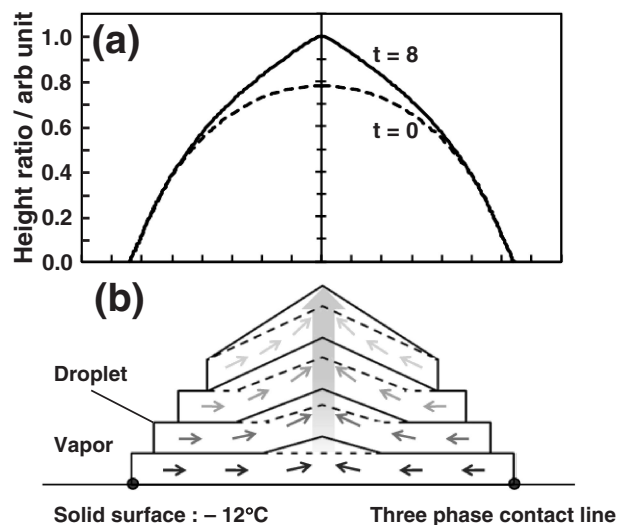


**Figure 5.** (a) Shape change of the droplet before and after freezing, and (b) schematic illustration of the freezing behavior on the FAS-3-coated surface.

temperature was  $-12.0\text{ }^{\circ}\text{C}$  and a water droplet was placed on the sample surface, the droplet was frozen; the top of the droplet was sharpened like an onion after the completion of freezing. Based on the results of the freezing ratio at each time and the volume ratio at each height, it is conceivable that freezing of the droplet initiated from the three-phase contact line and that it advanced linearly in the vertical direction.

This research was supported in part by JSPS Research Fellowship No. H22-8538.

#### References and Notes

- M. Miwa, A. Nakajima, A. Fujishima, K. Hashimoto, T. Watanabe, *Langmuir* **2000**, *16*, 5754.
- A. B. D. Cassie, S. Baxter, *Trans. Faraday Soc.* **1944**, *40*, 546.
- A. Nakajima, A. Fujishima, K. Hashimoto, T. Watanabe, *Adv. Mater.* **1999**, *11*, 1365.
- R. N. Wenzel, *Ind. Eng. Chem.* **1936**, *28*, 988.
- T. Furuta, M. Sakai, T. Isobe, A. Nakajima, *Langmuir* **2010**, *26*, 13305.
- S. Suzuki, A. Nakajima, N. Yoshida, M. Sakai, A. Hashimoto, Y. Kameshima, K. Okada, *Langmuir* **2007**, *23*, 8674.
- S. Suzuki, A. Nakajima, N. Yoshida, M. Sakai, A. Hashimoto, Y. Kameshima, K. Okada, *Chem. Phys. Lett.* **2007**, *445*, 37.
- P. Tourkine, M. L. Merrer, D. Quéré, *Langmuir* **2009**, *25*, 7214.
- Supporting Information is available electronically on the CSJ-Journal Web site, <http://www.csj.jp/journals/chem-lett/index.html>.